New insights into mid-late Pleistocene fossil hominin paranasal sinus morphology

Zollikofer, C P E ; Ponce de León, M S ; Schmitz, R W ; Stringer, C B

DOI: https://doi.org/10.1002/ar.20779

THE ANATOMICAL RECORD 000:000–000 (2008)

New Insights Into Mid-Late Pleistocene Fossil Hominin Paranasal Sinus Morphology

CHRISTOPH P.E. ZOLLIKOFER,[1]* MARCIA S. PONCE DE LEÓN,[1] RALF W. SCHMITZ,[2] AND CHRISTOPHER B. STRINGER[3]

[1]Anthropological Institute, University of Zurich, Zurich, Switzerland
[2]Universität Tübingen, Institut für Ur- und Frühgeschichte, Tübingen, Germany
[3]Department of Palaeontology, The Natural History Museum, London, England

ABSTRACT

Mid-late Pleistocene fossil hominins such as *Homo neanderthalensis* and *H. heidelbergensis* are often described as having extensively pneumatized crania compared with modern humans. However, the significance of pneumatization in recognizing patterns of phyletic diversification and/or functional specialization has remained controversial. Here, we test the null hypothesis that the paranasal sinuses of fossil and extant humans and great apes can be understood as biological spandrels, i.e., their morphology reflects evolutionary, developmental, and functional constraints imposed onto the surrounding bones. Morphological description of well-preserved mid-late Pleistocene hominin specimens are contrasted with our comparative sample of modern humans and great apes. Results from a geometric morphometric analysis of the correlation between paranasal sinus and cranial dimensions show that the spandrel hypothesis cannot be refuted. However, visualizing specific features of the paranasal sinus system with methods of biomedical imaging and computer graphics reveals new aspects of patterns of growth and development of fossil hominins. Anat Rec, 000:000–000, 2008.

Key words: paranasal sinus; fossil; hominins

During the past years, a growing number of studies have been focusing on the structure and function of paranasal sinuses in great apes, living humans, and fossil hominins. Patterns of presence/absence of sinuses in different taxonomic groups, as well as patterns of morphological variability within groups, are now documented at a high level of comprehensiveness and detail and give interesting insights into the complex evolutionary history of these structures. Intriguingly, however, basic questions relating to the why and wherefore of pneumatization remain largely unanswered.

The fact that sinus morphology is difficult to interpret, and that sinus function remains elusive, has various reasons. One major reason is the morphological complexity and remarkable diversity displayed by one and the same structure within any given taxon, and even between left and right sides of any given individual. This makes it difficult to quantify and compare sinus morphology beyond measurements of volume and overall extension. Another reason is the remarkable diversity of functional hypotheses proposed with regard to pneumatization. Relating sinus function to otic and respiratory physiology, biomechanics, and climate is often plausible, but empirical evidence for or against specific hypotheses remains equivocal, such that alternative hypotheses cannot be corroborated with convincing evidence.

Structure, development, function, and evolution of sinuses are currently investigated with various methods. Structure is best investigated using computed tomography (CT) as a noninvasive imaging tool to document and quantify within and between taxon variability, as well

*Correspondence to: Christoph P.E. Zollikofer, Anthropological Institute, University of Zurich, Winterthurerstrasse 190, CH-8057 Zurich, Switzerland. Tel.: +41-44-635-5427. Fax: +41-44-635-6886. E-mail: zolli@aim.uzh.ch

Received • • •; Accepted • • •.

DOI 10.1002/ar.20779
Published online 00 Month 2008 in Wiley InterScience (www.interscience.wiley.com).

AQ2

J_ID: Z3X Customer A_ID: 08-0121 Cadmus Art: AR20779 Date: 22-SEPTEMBER-08 Stage: I Page: 2

as developmental change (Wind, 1984; Koppe and Ohkawa, 1999; Chaiyasate et al., 2007). Moreover, computer simulations of sinus morphogenesis can be used as model systems to better understand the basic principles of pneumatization (see companion article). Functional hypotheses, on the other side, are best tested against a generalized null hypothesis, stating that pneumatization is most parsimoniously seen as a biological spandrel *sensu* Gould and Lewontin (1979). From this perspective, air-filled spaces represent a spatial compromise at the interface between different functional/developmental compartments of the cranium rather than structures adapted to a specific function. Following this line of argument, mucous tissue of the nasopharyngeal cavity opportunistically invades adjacent intraosseous compartments, occupying the available space while obeying biomechanical minimum conditions (Sherwood, 1999).

Finally, questions relating to the evolution of air-filled spaces are best addressed with comparative studies of extant and fossil specimens (Rae, 1999; Witmer, 1999; Rossie et al., 2002). In the hominin clade, only relatively few fossil specimens are available, such that assessment of intra- versus interspecific variability and phyletic interpretation are challenging tasks. Even worse, most specimens are fragmentary, such that it is often impossible to relate paranasal sinus morphology to overall cranial morphology. Interestingly, since the very beginnings of human paleontology, the morphology of paranasal sinuses was used as an argument for or against the specific taxonomic status of fossil hominins. For example, in a discussion of the frontal sinus of the Neanderthal type specimen, Davis (1865) questions the taxonomic relevance of this feature because, in modern humans, sinuses are "liable to variation," and no apparent correlation exists between frontal sinus morphology and the external aspect of the glabellar region.

Neanderthals have always been the cornerstone during the discussion of paranasal air spaces in fossil hominins. While cranial pneumatization is typically believed to have been reduced during the evolution of the genus *Homo* (Sherwood et al., 2002), Neanderthal crania are often described as heavily pneumatized (Heim, 1974, 1997). In fact, their remarkable facial and nasal morphology exhibits a suite of traits, which have been considered autapomorphic, and associated with cold adaptation (Coon, 1962), special respiratory functions (Schwartz and Tattersall, 1996), and with biomechanical constraints during mastication and paramasticatory functions (Rak, 1986; Demes, 1987).

Studies focusing explicitly on the paranasal sinus morphology of fossil hominins essentially adopt the same set of baseline arguments to identify specific morphological traits and possible functional contexts. For example, in an analysis of cranial pneumatization in mid-Pleistocene *Homo* specimens, various features of the sinus system are described as unique (Seidler et al., 1997), and a geometric–morphometric analyses of internal and external sagittal vault profiles establishes potential relationships between shape and biomechanical constraints (Prossinger et al., 2000; Ravosa et al., 2000). On the other side, a recent study of temporal pneumatization in Asian *H. erectus* supports the notion that patterns of pneumatization are highly variable and constrained only by the morphology of the temporal bone (Balzeau and Grimaud-Hervé, 2006).

The aim of the present study is to add to the empirical evidence of paranasal sinus morphology in fossil hominins and in a comparative sample of extant humans and great apes. Rather than seeking evidence for potentially apomorphic traits and specific functional contexts, we look at sinus morphology from the perspective of the "spandrel" null hypothesis. To test this hypothesis, we follow a double approach. First, we provide detailed descriptions of sinus morphology in a sample of well-preserved mid-late Pleistocene hominin specimens and ask whether paranasal sinus morphology in this sample differs substantially from sinus morphology in our comparative sample of modern humans and great apes. Second, using methods of geometric morphometrics, we ask whether sinus form can be explained statistically as a function of cranial form. In both cases, the null hypothesis can be rejected if the fossil hominin sample stands out of general patterns of covariation between sinus morphology and cranial morphology. Finally, we provide a tentative interpretation of our findings in terms of possible developmental and/or functional factors influencing the morphology of the paranasal sinus system.

MATERIALS AND METHODS

Fossil Sample

The fossil hominin sample consists of six adult Neanderthal specimens (Gibraltar 1 [Forbes' Quarry], Tabun C1, La Ferrassie 1, Amud 1, Neanderthal-type specimen [Kleine Feldhofer Grotte], and Spy1), and the Broken Hill specimen, which is typically attributed to *Homo heidelbergensis* or archaic *H. sapiens*. In the Forbes' Quarry specimen, the entire paranasal sinus system is preserved, but partially filled with coarse-grained limestone breccia (as was the nasal cavity prior to preparation). Sediments are still present in the right maxillary sinus, in many of the ethmoid air cells, and along the medial wall of the left maxillary sinus. The right maxilla exhibits some damage on its lateral and posterior sides, and the right orbital floor is eroded. Most of the left maxillary sinus, as well as the frontal and sphenoid sinuses, are free of sediment and in good state of preservation. To stabilize the thin bony walls of the left maxilla, the frontal, and the sphenoid, the respective sinuses were partially filled with plaster. During preparation and conservation of the specimen, the nasal cavity was partially freed from sediment. Close inspection of the lateral nasal walls shows breakage of lamellar bone, and the relative contribution of sediment and bone to the current surface structures remains unclear.

The cranial vault of the Neanderthal type specimen is almost complete but exhibits an anteroposterior crack, which was filled with plaster, probably shortly after the specimen's discovery. During this process, the frontal sinus was partially filled with plaster. Otherwise, the frontal sinus is almost completely preserved and exhibits only minor deterioration at the frontoethmoidal suture. The well-preserved left zygomatic bone contains a recess of the maxillary sinus. This bone, which clearly belongs to the Neanderthal type specimen, has a remarkable history. During the 1997 survey excavations in the Neander Valley, the original fillings of the Feldhofer Cave could be identified, and numerous stone artifacts, faunal remains, and hominin bones were recovered from the place where the fillings had been dumped in 1856. Fur-

ID: selvarajj Date: 22/9/08 Time: 16:58 Path: J:/Production/AR##/Vol00000/080160/3B2/C2AR##080160

J_ID: Z3X Customer A_ID: 08-0121 Cadmus Art: AR20779 Date: 22-SEPTEMBER-08 Stage: I Page: 3

ther excavations yielded a total of 73 hominin bone fragments, three of which matched the 1856 finds: the left zygomatic bone, a right temporal fragment, and a fragment of the left lateral femoral condyle (Schmitz et al., 2002; Smith et al., 2006).

Following CT data acquisition, the Tabun C1, Amud 1, and Spy 1 crania were decomposed electronically into isolated fragments and then reassembled on the computer screen following standard procedures. The basic aim of virtual reconstruction was to correct existing deformations, and to readjust the position and orientation of the facial parts relative to the neurocranium. These specimens exhibit similar patterns of deterioration: each of them suffered breakage in the area of the frontal sinuses, but basic sinus dimensions can be recovered with fair precision. The midfacial skeleton is fragmentary, such that information on the maxillary, ethmoid, and sphenoid sinuses is not available. The La Ferrassie 1 specimen was available as a cast, and frontal sinus dimensions were derived from the literature (Vlcek, 1967).

The Broken Hill cranium preserves the complete system of paranasal sinuses, with only minor damage to the orbital walls of the ethmoid, and to the right sphenoid sinus (which contains minor plaster fillings).

Comparative Sample of Extant Species

Modern humans are represented by a mixed-population sample (N = 10), comprising European, African, Patagonian, Inuit, and Australian crania, plus the cranium derived from the Visible Male data set. This sample was composed to represent wide diversity in paranasal sinus morphology and cranial shape. The great ape sample consists of mixed-population subsamples of *Pan troglodytes*, *Gorilla gorilla*, and *Pongo pygmaeus*. Each species is represented by N = 8 specimens (four females, four males). Specimens are from the collections of the Anthropological Institute, University of Zurich; the Royal Africa Museum, Tervuren (Belgium); and the Bayrische Staatssammlungen, München.

Data Acquisition and Processing

Digital volume data of all specimens were acquired with medical CT. The average spatial resolution of the reconstructed images is 0.3 mm per voxel in *x*,*y*,*z* directions. Because of the high X-ray density of the Broken Hill cranium, the extended Hounsfield scale option was applied to produce cross-sectional images resolving the full range of density variation in this specimen.

CT data acquisition of the paranasal sinuses requires special tuning of imaging parameters, because bony lamellae between air-filled cells and lobes are typically thinner than the minimum spatial resolution of medical CT scanners. Because of the resulting partial volume effects, these structures are imaged at lower than actual X-ray densities. This effect was taken into account during data segmentation by prefiltering images with a high-pass filter, thus enhancing the contrast between small-scale structures and the surrounding air. To extract the paranasal sinus volumes from the surrounding bone, we used interactive flood-fill segmentation algorithms implemented in the software package Amira (Konrad-Zuse-Zentrum für Informationstechnik, Berlin). In the fossil specimens, sediment and plaster fillings were removed electronically prior to segmentation of the sinus volume.

Data Visualization

Traditionally, sinuses are visualized as solid volumes within transparent bone. Alternatively, for better visibility, a virtual window is cut into the bone to see the sinuses contained in the bone (Koppe and Ohkawa, 1999). However, because bony surfaces are visualized in front of the sinuses or removed entirely, it is often difficult to assess the exact spatial relationships between air-filled spaces and the surrounding bone. We thus use an alternative visualization paradigm: taking into account the fact that sinuses represent intraosseous compartments, it is most informative to visualize them as solid objects contained within bony walls, while removing the wall directed toward the observer. This can be achieved by digitally removing all surfaces oriented toward the observer (Fig. 1). This procedure renders sinuses as filled spaces seen from outside, and bony surfaces as seen from inside. F1

Morphometric Analysis

Here, we concentrate on correlations of frontal sinus dimensions with cranial size and shape. Frontal sinus form was quantified by its maximum extensions in the three main anatomical directions: mediolateral (width), caudocranial (height), and anteroposterior (depth), as defined by Vlcek (1967). As a proxy for frontal sinus size S_f, we used the geometric mean of these three measurements (*P. pygmaeus* does not exhibit a frontal sinus proper, but the respective interorbital space is occupied by superior recesses of the maxillary sinuses (Koppe and Ohkawa, 1999), which are present in all specimens of our sample). Although direct sinus volume measurements are technically feasible, the volume strongly depends on the development of individual fingering patterns (see paper on sinus morphogenesis), while S_f is a good indicator of the maximum dimensions of the sinus in all three directions of space.

Cranial form was quantified by 80 three-dimensional external and internal cranial landmarks, defining locations of homology between all crania in the sample. Form variability in the sample was analyzed with principal components analysis (PCA) of shape (Dryden and Mardia, 1998). Following calculation of cranial centroid size S_c for each specimen, specimens are normalized to centroid size $S = 1$ and superimposed with generalized least-squares fitting (Rohlf and Slice, 1990). Shape variation in the sample can then be decomposed into a suite of statistically independent factors of shape variation (i.e., principal, PCs) accounting for the largest, second largest, etc. proportions of the total shape variability in the sample. Typically, the first few PCs account for a high proportion of the total variability, such that higher-order PCs can be omitted without loss of significant morphometric information.

To evaluate the relationship between sinus size and cranial size, $\log(S_f)$ was regressed on $\log(S_c)$. The residuals of this allometric regression function quantify variation in sinus size independent of variation in cranial size and can thus be used as a measure of sinus shape

ID: selvarajj Date: 22/9/08 Time: 16:58 Path: J:/Production/AR##/Vol00000/080160/3B2/C2AR##080160

J_ID: Z3X Customer A_ID: 08-0121 Cadmus Art: AR20779 Date: 22-SEPTEMBER-08 Stage: I Page: 4

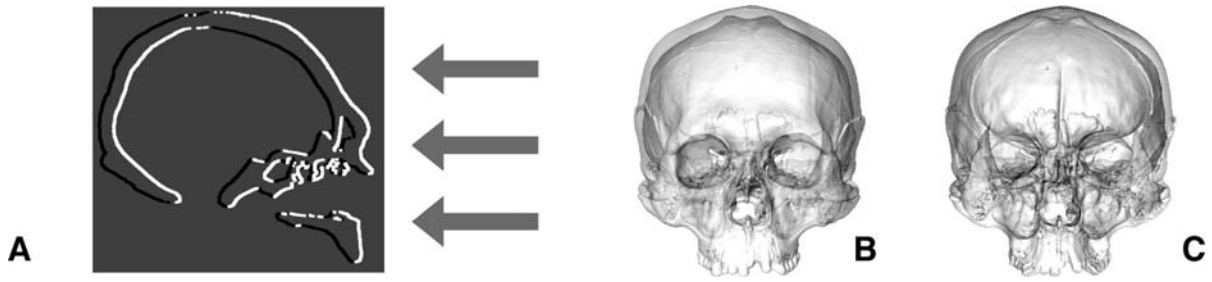

Fig. 1. Visualization paradigm for endocranial cavities. **A**: During traditional rendering, only those surfaces are visualized whose normals point toward the observer (white). During cavity rendering, only those surfaces are visualized, whose normals point away from the observer (black). **B**: traditional rendering. **C**: Cavity rendering. Note that sinuses appear as filled spaces, whereas the surrounding bone appears as a cavity. This facilitates assessment of the spatial relationships between sinuses and bony boundary structures.

S_f. In the following step, S_f was regressed against cranial shape. This was done for each PC separately (because of the inhomogeneous distribution of species subsamples in shape space, multivariate regression of sinus shape on all cranial shape PCs cannot be used here). Significant patterns of covariation between cranial and sinus shapes were visualized by means of cranial shape transformation, using methods described elsewhere (Zollikofer and Ponce de León, 2002).

RESULTS

Morphological Observations

Forbes' Quarry. Compared with other Neanderthals, such as the type specimen and the Amud cranium, the Forbes' Quarry cranium is relatively lightly built, with only moderate facial superstructures. In congruence with its external morphology, the pneumatization of the face is also relatively moderate (Fig. 2A). The system of ethmoid air cells is confined to the interorbital space and does not invade the supra- and postorbital areas, as in other Neanderthal specimens (see later), but the crista galli contains a well-developed air cell. As a whole, the ethmoid air cells occupy a relatively low but anteroposteriorly extended space in the cranium, in correspondence with the elongated orbital cavities typical for the Neanderthals. The sphenoid sinus consists of three compartments, all confined to its body and not extending toward the greater wing. A relatively narrow central air cell, which originates from the left sphenoid concha, occupies the space between the sellar and the inferior faces of the sphenoid body, and partially invades the basioccipital through the spheno-occipital synchondrosis. Two lateral cells, originating from the left and right conchae, respectively, extend toward the infratemporal fossae. The frontal exhibits pronounced asymmetry. On its right side, it extends until above the supraorbital notch and ramifies into several lobes. On its left side, it is essentially confined to the glabellar region. Because the left supraorbital region is damaged, sediment filling of the lateral parts of the left frontal sinus must be taken into consideration. However, CT-based analysis of the bone structure in this region shows no evidence of sinus walls, which typically appear as dense rims on CT images, exhibiting higher X-ray absorption than cancellous bone. The well-preserved left maxillary sinus exhibits formation of lobes around the infraorbital canal; likewise, the zygomatic recesses are well developed and extend beyond the maxillozygomatic suture into the zygomatic bone. In lateral view, this sinus has an elongated shape, reflecting the anteriorly extended shape of the Neanderthal midface.

Neanderthal type specimen. Compared to the robust external appearance and well-developed supraorbital torus and glabellar eminence of this cranium, the frontal sinus exhibits only moderate development in both lateral and superior directions (Fig. 2B). The left zygomatic bones contains two deep recesses of the maxillary sinus, which intrude into the maxillary process of this bone well beyond the maxillozygomatic suture and reaching the level of the zygomatico-orbital foramina.

Spy 1, Tabun C1, Amud 1. Although the supraorbital region in these specimens is heavily damaged, it is possible to reconstruct the overall dimensions (width, height, depth) of the frontal sinus. Like in the Neanderthal type specimen, the frontal sinus in these three specimens is wider than high, extending laterally toward the highest points of the orbits.

Broken Hill. The sinus system of this robust specimen is well developed (Fig. 2C). The ethmoid sinus is wide mediolaterally, corresponding to the wide interorbital distance. It extends laterally into the supraorbital area of the frontal bone, forming sheet-like lobes that intrude into the thin diploic region between the medial orbital roofs and the floor of the anterior cranial fossa. The frontal sinus also exhibits two sheet-like extensions into the superior orbital region. The squamous portion of the frontal sinus is conspicuous. It consists of finger-like lobes extending into the frontal squamae while closely following the shape of the internal table. This fan-like structure has additional, mushroom-like extensions protruding anteriorly into the supraorbital torus, and notably into the glabellar eminence. Like in Forbes' Quarry, the frontal sinus exhibits considerable asymmetry. Here, the left side extends until the lateral orbital rim, while the right side does not extend beyond the supraorbital notch. The sphenoid sinus compartment is

ID: selvarajj Date: 22/9/08 Time: 16:58 Path: J:/Production/AR##/Vol00000/080160/3B2/C2AR##080160

J_ID: Z3X Customer A_ID: 08-0121 Cadmus Art: AR20779 Date: 22-SEPTEMBER-08 Stage: I Page: 5

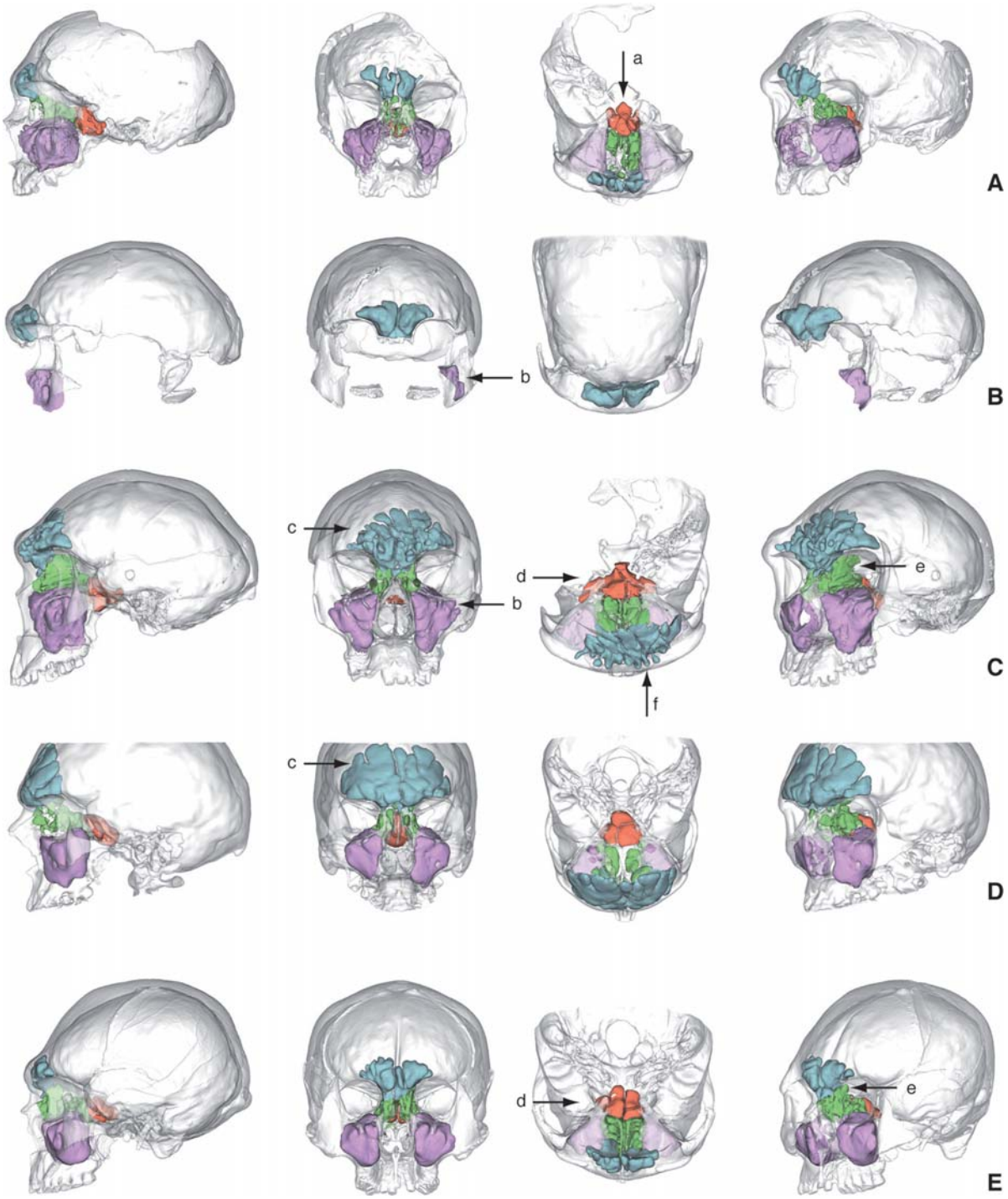

COLOR

Fig. 2. Paranasal sinus morphology in fossil and modern humans. **A**: Forbes' Quarry (Gibraltar 1) Neanderthal. **B**: Neanderthal-type specimen. **C**: Broken Hill specimen. **D**: Modern human (visible human data set, male individual). **E**: Modern human (Ona, Tierra del Fuego, Natural History Museum, London, spec. #1933.6.15.1). Specimens are oriented in the Frankfurt plane and shown (from left to right) in left lateral, frontal, superior views, and at an angle of 45 degree off the midsagittal plane. All internal surfaces are oriented toward the observer, and external surfaces are not visualized. Color codes: green: ethmoid sinus; orange: sphenoid sinus; blue: frontal sinus; violet: maxillary sinuses. Arrows: **a**: tripartite sphenoid sinus; **b**: double recess of maxillary sinus into zygomatic bone; **c**: squamous frontal sinus; **d**: expansion of sphenoid sinus into greater wing; **e**: ethmoid (and frontal) sinus lobes in orbital roof; **f**: anterior expansion of frontal sinus.

ID: selvarajj Date: 22/9/08 Time: 16:58 Path: J:/Production/AR##/Vol00000/080160/3B2/C2AR##080160

J_ID: Z3X Customer A_ID: 08-0121 Cadmus Art: AR20779 Date: 22-SEPTEMBER-08 Stage: I Page: 6

comparatively short anteroposteriorly, but exhibits lateral lobes that extend around the posterior region of the orbital cavities, and intrude into the greater wings of the sphenoid. This latter condition was described as unique (Seidler et al., 1997), but it is also found in modern humans (Terra et al., 2006). The maxillary sinuses exhibit a lobed structure, wrapping around various internal bony crests, which correspond to the canal for the anterior superior alveolar nerve and vessels and its ramifications, as well as to the canal of the zygomaticofacial nerve and vessels.

Modern humans. Figure 2D,E shows the paranasal sinus morphology of two human crania, both of which are comparatively large and robust. These specimens were chosen to illustrate within-species variability in the relationship between superstructures and endocranial cavities. Interestingly, the comparatively robust Ona (Tierra del Fuego) specimen (Fig. 2E) has a less-developed frontal sinus than the visible human (Fig. 2D). As a qualitative observation, it may be stated that the presence of a strong glabellar prominence and associated supraglabellar depression is often correlated with absence of a frontal squamous sinus in modern humans. Conversely, formation of a squamous sinus is accompanied by anterior bulging of the external table of the frontal bone, which levels out the supraglabellar depression.

Correlation of Frontal Sinus Form With Cranial Form

According to our null hypothesis, it can be expected that the form of ethmoid, sphenoid, and maxillary sinuses essentially reflects the form of the available spatial compartments that are formed as a consequence of differential developmental trajectories of the neurocranium and viscerocranium. The frontal sinus assumes a somewhat special position. Development of the outer table of the frontal squama is less constrained—both functionally and developmentally—than that of other cranial regions containing sinuses. Assuming that sinuses are more than spandrels, it can thus be expected that the frontal sinus is the most likely candidate to show correlation between form and specific sinus function, and that its form is only weakly related to developmental and functional constraints of the cranium as a whole. Analyzing correlations between frontal sinus form and cranial form is thus the most sensitive test of the spandrel null hypothesis.

The results of correlation analyses between frontal sinus dimensions and cranial dimensions are shown in Figs. 3 and 4. Sinus size S_f is related to cranial size S_c with a positive allometric coefficient (2.473), and the slope of the log-linear regression function is different from zero (Fig. 3B). The residuals of this regression function, which serve as a proxy for sinus shape S_f, were then tested for correlation with all PCs resulting from PCA of shape. Significant correlations could only be found with PC2 (Fig. 3C). Because PC2 itself is not correlated with cranial size, it represents a mode of shape variation, which influences frontal sinus shape independent of cranial size, and independent of taxon.

Figure 4 shows actual spatial patterns of shape variation corresponding to PC1 and PC2. PC1 basically expresses shape transformation from an average great ape cranium to an average modern human cranium (Fig. 4A). Beside the obvious pattern of neurocranial expansion and viscerocranial reduction characteristic of modern humans compared to the great apes, Fig. 4A reveals why the great ape-to-human transformation is not correlated with changes in S_f: facial shape change is best characterized as a "rotation" of the midface around glabella. Since the position of glabella remains fixed relative to the endocranial cavity, frontal sinus shape is not affected. Shape transformation corresponding to PC2 (Fig. 4B) can be characterized as a "rotation" of the

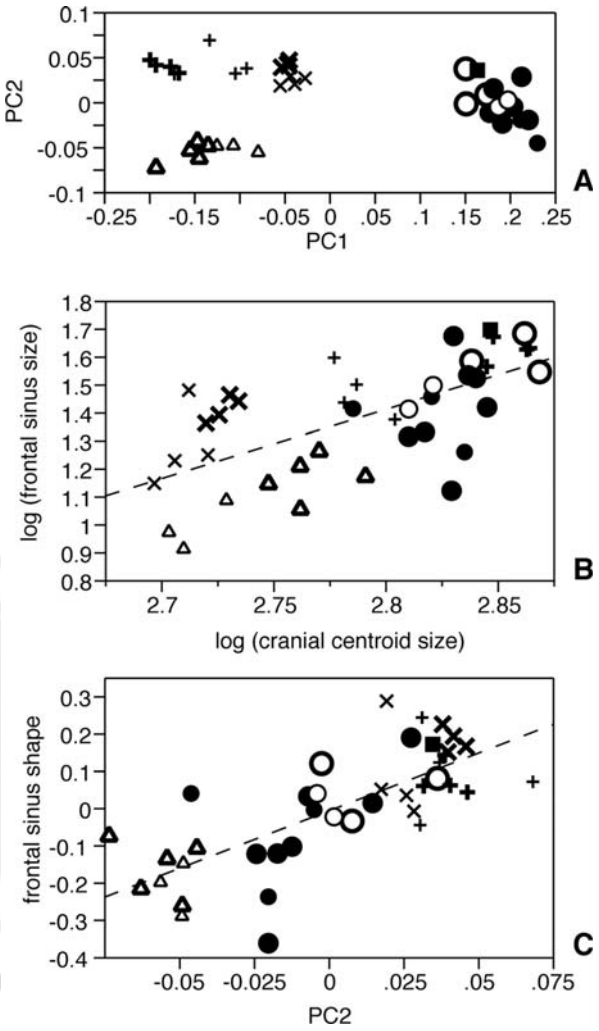

Fig. 3. Correlation between frontal sinus shape and cranial shape I: **A**: Cranial shape variability in a sample of hominins and Great Apes (filled circles: H. sapiens; open circles: Neanderthals; square: Broken Hill specimen; x: *P. troglodytes*; +: *G. gorilla*; triangles: *P. pygmaeus*; large/small symbols: males/females). **B**: Double logarithmic regression of frontal sinus size S_f against cranial centroid size S_c ($\log S_f = -5.514 + 2.473 \log S_c$; $r^2 = 0.43$; $P < 0.0001$). **C**: Double-logarithmic regression of frontal sinus shape S_f (the residuals of the regression function in B) against cranial shape component PC2 ($S_f = -0.0088 + 3.0890$ PC2; $r^2 = 0.56$; $P < 0.0001$).

ID: selvarajj Date: 22/9/08 Time: 16:58 Path: J:/Production/AR##/Vol00000/080160/3B2/C2AR##080160

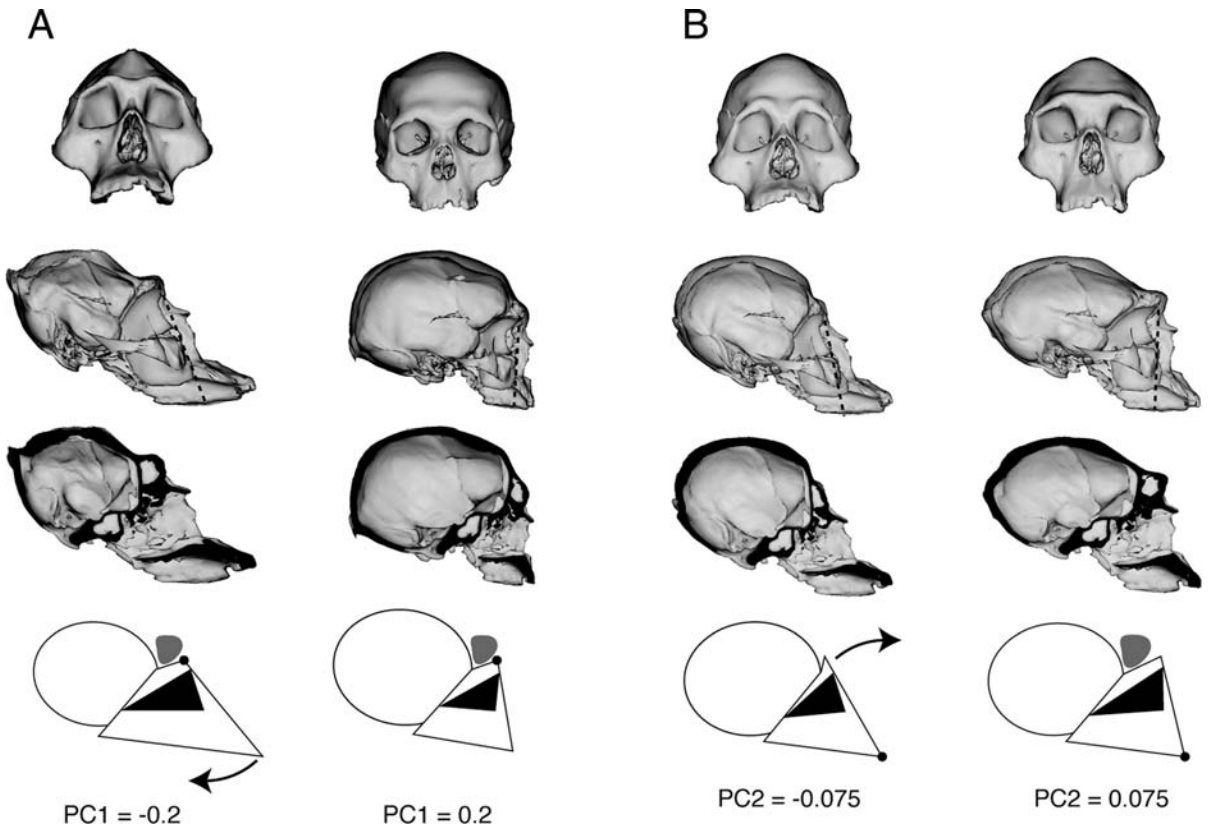

Fig. 4. Correlation between frontal sinus shape and cranial shape II: visualization of modes of shape variability. **A**: shape variability along PC1 (Fig. 3A) corresponds to transformation of an average human cranium (left; PC1 = −0.2) into an average great ape cranium (right, PC1 = 0.2). **B**: shape variability along PC2 (Fig. 3A,C) corresponds to transformation of an average human/ape specimen with a small frontal sinus (left, PC2 = −0.075) into an average human/ape specimen with a large frontal sinus (right, PC2 = 0.075). Stippled lines indicate orientation of orbital plane. Line graphs summarize major shape differences (ellipse: braincase; quadrangle: face; black triangle: orbital cavity; gray blob: frontal sinus): In **A**, the midface is shortened by "rotation" of the facial complex around glabella (black circle); sinus size remains constant. In **B**, the upper face is advanced by "rotation" of the facial complex around prosthion (black circle). Note reorientation and elongation of orbital cavities, as well as widening of interorbital space (see top graph of B).

upper face away from the neurocranium, with prosthion as a fixed point. As a result, glabella advances toward a more anterior position, giving rise to an intrafrontal space, which is occupied by the frontal sinus. Simultaneously, the interorbital space is widened, giving additional space for sinus development. This pattern essentially describes transition from an *Pongo*-like to an African ape-like cranial morphology, but it is worth noting here that hominins exhibit considerably more variation along PC2 (i.e., in facial relative to neurocranial orientation) and, correspondingly, in sinus shape, than each of the great ape species. This point will be discussed in more detail later. Overall, shape transformation corresponding to PC2 indicates that frontal sinus shape is primarily determined by the orientation and shape of the upper face (specifically the orbital cavities) relative to the neurocranium.

Interestingly, modes of shape variation corresponding to PC1 and PC2 are both associated with variation in facial relative to neurocranial orientation, which is typically described in terms of facial kyphosis. PC1 depicts transition from the more airorhynch great apes (upward-oriented face) to the more klinorhynch hominins (downward-oriented face), while PC2 depicts transition from airorhynch *Pongo* to more klinorhynch *Gorilla* and *Pan* morphologies. Our results show that facial kyphosis is a descriptive category, which is not sufficiently precise to account for the multifactorial phyletic and developmental basis of variation in facial relative to neurocranial orientation and position.

DISCUSSION

Hominin fossils have often been described as having extended paranasal sinuses (Weidenreich, 1943; Seidler et al., 1997), but since the very beginnings of paleoanthropology, the idea that air-filled spaces may have taxon-specific morphologies was received with scepticism (Davis, 1865). The basic question is whether sinus form results from the general scaling laws of the hominoid cranium, or whether other explanatory factors, such as phyletic grade shifts in sinus morphology (Rae, 1999), or

specific sinus function, need to be advocated as explanatory factors. Empirical evidence from studies of higher primates and humans tends to support the former view. For example, in anthropoid primates, the size of the maxillary sinus appears to be primarily determined by facial dimensions (Koppe et al., 1999; Rae and Koppe, 2000), and this is true even when sinus size demonstrably depends on external factors: A comparison of different populations of the Japanese macaque, *Macaca fuscata*, showed that sinus volume decreases with decreasing mean annual temperature, but that this is a side effect of expansion of the nasal cavity (Rae et al., 2003).

The analyses presented here support the notion that sinus morphology in fossil hominins follows the general trends found in hominoid primates, and that potential peculiarities of their sinus system basically reflect taxon-specific features of their craniofacial morphology. However, because the craniofacial morphology of fossil hominins is clearly distinct from that of modern humans, examination of their sinus morphology provides new insights into processes of phyletic diversification and of cranial growth and development.

Comparison of the paranasal sinus morphology in the fossil and modern human sample of this study shows that variability in the fossil sample is considerable, both qualitatively and quantitatively, but not greater than in modern humans (Figs. 2 and 3). Most importantly, all pneumatic variants seen in the fossil hominin sample can also be found in modern humans, although they tend to occur at lower frequencies (Weiglein, 1999). For example, pneumatization of the orbital roof through recesses of the ethmoid and/or frontal sinus is common in fossil hominins, but also in modern humans (Weiglein, 1999), while pneumatization of the sphenoid wing is a relatively rare but nonsymptomatic condition in modern humans (Terra et al., 2006). Overall, clinical case studies show that (pathological) pneumatization can, in principle, affect all cranial bones, including the parietals, occipital, and nasal conchae (Littrell et al., 2004; Rebol et al., 2004).

Neanderthals assume an important place in the discussion of sinus morphology, because the notion that Neanderthals are heavily pneumatized has almost reached textbook status of knowledge (Laitman et al., 1996; Rae and Koppe, 2004). However, as pointed out by Vlcek in his comprehensive comparative study of Neanderthal frontal pneumatization, this hypothesis cannot be upheld (Vlcek, 1967). This author characterizes Neanderthal frontal sinuses as cauliflower-shaped cavities occupying large parts of the supraorbital region, which are relatively uniform in structure, compared to the highly variable frontal sinuses of modern humans. He concludes that variation in sinus morphology closely follows evolutionary reorganization of the supraorbital area: while the frontal sinus of Neanderthals is confined to the region behind the browridges and does not extend into the moderately sloping frontal squama, pneumatization in modern humans tends to invade the steeply raising frontal squama.

Our data also confirm that, when related to craniofacial anatomy, Neanderthal paranasal pneumatization is not above human standards (Figs. 2 and 3). However, there are subtle differences in sinus shape. Compared to modern humans, the maxillary and ethmoid sinuses of the Gibraltar 1 specimen have an elongated shape, and the maxillary sinus a bulging anterior surface. This peculiar morphology reflects the elongated midfacial architecture of Neanderthals (note the long orbital cavities in Fig. 2A), and matches the shape of the facial surface of the Neanderthal maxilla. The morphology of the latter area is often described as "inflated," such that the question arises whether the bulging maxillae are formed through "hyperpneumatization," or whether their specific shape entails hyperpneumatization. Examination of the midfacial morphology of immature Neanderthal specimens shows that the latter scenario is the more likely explanation. Even in the youngest well-preserved Neanderthal specimen, the Mezmaiskaya neonate (Golovanova et al., 1999), the facial surface of the maxilla is large compared to modern human neonates (personal observation). The size of this surface is constrained by the position of the alveolar process of the maxilla relative to the orbits rather than by the size of the developing maxillary sinus. Similarly, expansion of the maxillary sinus into the zygomatic bone, as seen in the Forbes' Quarry, Neanderthal, and Broken Hill specimens (Fig. 2A–C), seems to be a consequence of the comparatively large zygomaticomaxillary interface. Zygomatic recesses are well developed in the great apes, such that we assume that this morphology represents the plesiomorphic condition in the hominoids.

The morphology of the frontal sinus of the Broken Hill specimen conserves valuable clues about the craniofacial development on the ontogeny of pneumatization in this individual. Left–right asymmetry of the frontal sinus (Fig. 2C) indicates that invasion of the frontal squama from the respective left and right anterior ethmoid air cells represented two independent growth processes. The fact that similar spatial constraints and physiological conditions of growth led to strikingly different morphologies in one and the same individual shows that sinus formation has an important stochastic component.

The fan-like extension of the sinus into the frontal squama contrasts with finger-like anterior extensions into the glabellar region. We hypothesize that formation of the squamous and glabellar portions of the frontal sinus corresponds to two successive growth processes of the face. As can be seen in modern humans, pneumatization of the frontal squama presupposes a steep orientation of the frontal squama relative to the orbits (Vlcek, 1967) (Fig. 2D vs. 2E). We suppose that, in Broken Hill, a similar spatial relationship between the orbits and the frontal squama existed during childhood and allowed its pneumatization. On the other hand, anterior growth of the sinus into the glabellar region is indicative of a later morphogenetic process associated with substantial facial advancement relative to the neurocranium, and formation of a prominent browridge. We suppose that this process took place relatively late during development, and that it might have been related to the development of sexual dimorphism. Similar considerations might apply to the Petralona cranium, which also exhibits a large, fan-like squamous frontal sinus, and pneumatization of the glabellar region by finger-like protrusions (Seidler et al., 1997).

The spandrel null hypothesis predicts, in its quantitative form, that pneumatization is largely an effect of cranial developmental allometry. Because the face and the braincase grow with positive and negative allometric coefficients, respectively (Ponce de León and Zollikofer,

TABLE 1. Allometry of frontal sinus size

	Exponent	SE	R^2	P
Cranium	2.47	0.46	0.43	<0.0001
Face	1.08	0.32	0.23	<0.0017
Neurocranium	1.37	0.34	0.30	<0.0003

Values represent allometric exponent SE, coefficient of determination, and levels of significance of regression equations relating $\log_{10}$ frontal sinus size S_f to $\log_{10}$ centroid size of the cranium (S_c), the face, and the neurocranium.

2001), nonfunctional spaces between various cranial compartments must be bridged in some way to guarantee biomechanical and structural coherence. But even nonfunctional spandrels are submitted to evolutionary optimization, such that formation of intraosseous air-filled volumes can be seen as a strategy to minimize material investment while maximizing biomechanical stability, similar to the formation of cortical, cancellous and marrow-filled compartments in long bones. Overall, thus, sinuses can be expected to reflect the position, orientation, and size of cranial compartments relative to each other rather than specific functions.

From this perspective, absence of sphenoid wing pneumatization in modern humans is an effect of the relatively large temporal and frontal lobes of the brain, which fills the respective regions between the temporal fossa and the orbits. Likewise, the bulging shape of the Neanderthal maxillary sinus reflects absence of a canine fossa, and presence of a large sinus expanding into the frontal squama of modern humans is related to their bulging forehead.

Combining our null hypothesis with the functional matrix hypothesis (Moss, 1986) led us to the proposition that frontal sinuses are less constrained by surrounding cranial compartments than other paranasal sinuses, and that they represent the best candidates to detect potential structure–function relationships. Figures 3 and 4 show that variation in frontal sinus size and shape can be explained statistically by variation in cranial size and shape. Similar results were obtained for the relationship between maxillary sinus dimensions and craniofacial dimensions in hominoid primates (Rae and Koppe, 2000). Both maxillary and frontal sinus sizes scale to cranial dimensions with a positive allometric coefficient. However, while maxillary sinus size scales isometrically with facial size (Rae and Koppe, 2000), our data suggest that frontal sinus size scales isometrically with neurocranial size, and allometrically with facial size (Table 1). T1

Correlation between cranial shape and sinus shape follows a more complex pattern. Transformation of an average great ape cranium into an average hominin cranium does not affect frontal sinus shape (Fig. 4A, PC1), because it mainly affects size, position, and orientation of the maxillae relative to the rest of cranium. The only cranial shape component exhibiting correlation with sinus shape was PC2, which captures major differences in facial orientation between Asian and African great apes, and also within modern humans (Fig. 4B). PC2 reflects change in facial orientation through rotation of the upper face around a fixed point near prosthion. This gives rise to an expanded supraorbital space, which, according to our data, is a precondition for extensive frontal pneumatization. As shown in Fig. 3C, modern humans exhibit greater variability along PC2 than Neanderthals or any of the great ape taxa and, as a consequence, frontal sinus dimensions are more variable than in the other hominoids. It is worth noting that PC2 not only reflects variation in facial orientation, but also in neurocranial shape, which changes from a more globular to a more elongated appearance (Fig. 4B). This pattern of correlated shape change corresponds to the transition from a brachycephalic to a dolichocephalic human cranium (Fig. 5). As shown earlier, this mode of variation is independent of age-related change in cranial shape. Rather, it seems to represent differences between individual morphotypes that are already formed at birth (Zollikofer and Ponce de León, 2002). It remains to be clarified why humans, compared to the Neanderthals and the great apes, exhibit more interindividual variation in the way in which the face is hafted to the braincase. A possible clue comes from the fact that the data scatter along PC2 not only characterizes a human mode of shape variation, but also captures major differences between Asian and African great ape morphologies. We hypothesize that this pattern of shape variation reflects a phyletically old mode of "developmental wobbling" in cranial shape, which governs both intra- and interspecific diversity. F5

Interestingly, the presence of a squamous frontal sinus has not been reported in Neanderthals, but it seems to

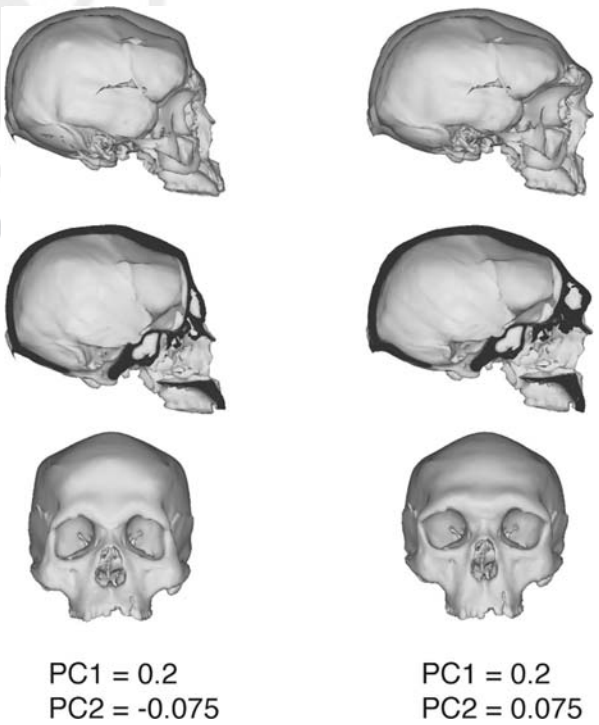

Fig. 5. Correlation between frontal sinus shape and cranial shape in hominins. Transformation of an average hominin cranium with a small frontal sinus (left; PC1 = −0.2, PC2 = −0.075) into an average hominin cranium with a large frontal sinus (right, PC1 = −0.2, PC2 = 0.075).

be a characteristic of *H. heidelbergensis* (as represented by the Broken Hill, Petralona and Steinheim specimens; (Prossinger et al., 2003)). It remains open whether co-occurrence of this feature in *H. heidelbergensis* and in modern humans represents homoplasy or homology. In the latter case, it could indicate evolutionary continuity between "archaic" and modern *H. sapiens*.

Taken as a whole, our data indicate that no specific functional hypotheses need to be advocated to explain variation in frontal sinus size and shape (note that there is no taxon-specific deviation from the regression line in Fig. 3C). Nevertheless, it is worth noting that only 56% of the total variation in sinus shape can be explained statistically by variation along cranial shape component PC2. We suppose that most of the remaining variation in sinus morphology can be understood as resulting from the essentially stochastic nature of sinus morphogenesis (see companion paper).

The basic developmental mechanism of paranasal sinus formation is expansion of nasal mucous epithelium into all surrounding bones "in an opportunistic manner within the constraints of a particular biomechanical loading regime" (Witmer, 1999). What might be called the "expansive tissue hypothesis" (see Zollikofer and Weismann, 2008, this issue) may serve here as a point of view from which sinus morphology in fossil hominins can be analyzed. One question that arises from the expansive tissue hypothesis is how cancellous diploic bone is replaced by mucous tissue. As can be seen in the frontal sinuses of the Broken Hill and Forbes' Quarry specimens, the less-developed sides of the sinuses extend toward regions of low trabecular density in the diploic layer. If this condition represents an incipient stage of sinus formation on this side, the following scenario can be hypothesized: rapid extension of the external table of the frontal bone combined with a low rate of deposition of extracellular bone matrix leads to thinning of the trabecular web, which in turn facilitates invasion of mucous epithelium and replacement of cancellous bone by air sacs. Furthermore, large intra- and interindividual variability between homologous sinuses indicates that the size and shape of air-filled regions is a function of the rate and duration of mucous tissue growth, and of the available space, which in turn depends on differential growth characteristics of the surrounding cranial compartments.

Further work will be needed to test these hypotheses in more detail. Nevertheless, while air-filled spaces in the cranium of fossil and extant hominoids might ultimately be best described as biological spandrels, it must be acknowledged that even spandrels reflect the architectural design codes imposed by evolution and development and thus constitute a rich source of information about differential modes of growth and development in fossil and extant hominins.

ACKNOWLEDGMENTS

We thank Sam Márquez for his invitation to contribute to this volume and for proofreading the manuscript. We thank Yoel Rak for granting access to fossil specimens, and Robert Krusynski (Natural History Museum London) and Isuf Hoxha for assistance with scanning.

LITERATURE CITED

Balzeau A, Grimaud-Hervé D. 2006. Cranial base morphology and temporal bone pneumatization in Asian *Homo erectus*. J Hum Evol 51:350–359.

Chaiyasate S, Baron I, Clement P. 2007. Analysis of paranasal sinus development and anatomical variations: a CT genetic study in twins. Clin Otolaryngol 32:93–97.

Coon CS. 1962. The origin of races. New York: Knopf.

Davis B. 1865. [Comments on]: The Neanderthal skull: its formation considered anatomically. J Anthropol Soc Lond 3:15–19.

Demes B. 1987. Another look at an old face: biomechanics of the Neandertal facial skeleton reconsidered. J Hum Evol 16:297–303.

Dryden IL, Mardia K. 1998. Statistical shape analysis. New York: Wiley.

Golovanova LV, Hoffecker JF, Kharitonov VM, Romanova GP. 1999. Mezmaiskaya cave: A Neanderthal occupation in the Northern Caucasus. Curr Anthropol 40:77–86.

Gould SJ, Lewontin RC. 1979. The spandrels of San Marco and the Panglossian paradigm: a critique of the adaptationist programme. Proc R Soc Lond B 205:581–598.

Heim JL. 1974. Les hommes fossiles de La Ferrassie (Dordogne) et le problème de la définition des Néanderthaliens classiques. L'Anthropologie 78:312–378.

Heim JL. 1997. Ce que nous dit le nez du néanderthalien. La Recherche 294:66–70.

Koppe T, Ohkawa Y. 1999. Pneumatization of the facial skeleton in catarrhine primates. In: Koppe T, Nagai H, Alt KW, editors. The paranasal sinuses of higher primates. Chicago: Quintessence. p 77–119.

Koppe T, Rae TC, Swindler DR. 1999. Influence of craniofacial morphology on primate paranasal pneumatization. Ann Anat 181:77–80.

Laitman JT, Reidenberg JS, Marquez S, Gannon PJ. 1996. What the nose knows: new understandings of Neanderthal upper respiratory tract specializations. Proc Natl Acad Sci USA 93:10543–10545.

Littrell LA, Leutmer PH, Lane JI, Driscoll CL. 2004. Progressive calvarial and upper cervical pneumatization associated with habitual valsalva maneuver in a 70-year-old man. AJNR Am J Neuroradiol 25:491–493.

Moss ML. 1986. Newer analytical models of craniofacial growth. Nova Acta Leopoldina NF 58:17–25.

Ponce de León MS, Zollikofer CPE. 2001. Neanderthal cranial ontogeny and its implications for late hominid diversity. Nature 412:534–538.

Prossinger H, Bookstein F, Schafer K, Seidler H. 2000. Reemerging stress: supraorbital torus morphology in the mid-sagittal plane? Anat Rec 261:170–172.

Prossinger H, Seidler H, Wicke L, Weaver D, Recheis W, Stringer C, Müller GB. 2003. Electronic removal of encrustations inside the Steinheim cranium reveals paranasal sinus features and deformations, and provides a revised endocranial volume estimate. Anat Rec B (New Anatomist) 237:132–142.

Rae TC. 1999. The maxillary sinus in primate paleontology and systematics. In: Koppe T, Nagai H, Alt KW, editors. The paranasal sinuses of higher primates. Chicago: Quintessence. p 177–189.

Rae TC, Hill RA, Hamada Y, Koppe T. 2003. Clinal variation of maxillary sinus volume in Japanese macaques (*Macaca fuscata*). Am J Primatol 59:153–158.

Rae TC, Koppe T. 2000. Isometric scaling of maxillary sinus volume in hominoids. J Hum Evol 38:411–423.

Rae TC, Koppe T. 2004. Holes in the head: evolutionary interpretations of the paranasal sinuses in catarrhines. Evol Anthropol 13. AQ1

Rak Y. 1986. The Neanderthal: a new look at an old face. J Hum Evol 15:151–164.

Ravosa MJ, Vinyard CJ, Hylander WL. 2000. Stressed out: masticatory forces and primate circumorbital form. Anat Rec 261:173–175.

Rebol J, Munda A, Tos M. 2004. Hyperpneumatization of the temporal, occipital and parietal bones. Eur Arch Otorhinolaryngol 261:445–448.

Rohlf FJ, Slice D. 1990. Extensions of the Procrustes method for the optimal superimposition of landmarks. Syst Zool 39:40–59.

Rossie JB, Simons EL, Gauld SC, Rasmussen DT. 2002. Paranasal sinus anatomy of Aegyptopithecus: implications for hominoid origins. Proc Natl Acad Sci USA 99:8454–8456.

Schmitz RW, Serre D, Bonani G, Feine S, Hillgruber F, Krainitzki H, Paabo S, Smith FH. 2002. The Neandertal type site revisited: interdisciplinary investigations of skeletal remains from the Neander Valley, Germany. Proc Natl Acad Sci USA 99:13342–13347.

Schwartz JH, Tattersall I. 1996. Significance of some previously unrecognized apomorphies in the nasal region of *Homo neanderthalensis*. Proc Natl Acad Sci USA 93:10852–10854.

Seidler H, Falk D, Stringer C, Wilfing H, Muller GB, zur Nedden D, Weber GW, Reicheis W, Arsuaga JL. 1997. A comparative study of stereolithographically modelled skulls of Petralona and Broken Hill: implications for future studies of middle Pleistocene hominid evolution. J Hum Evol 33:691–703.

Sherwood RJ. 1999. Pneumatic processes in the temporal bone of chimpanzee (*Pan troglodytes*) and gorilla (*Gorilla gorilla*). J Morphol 241:127–137.

Sherwood RJ, Ward SC, Hill A. 2002. The taxonomic status of the Chemeron temporal (KNM-BC 1). J Hum Evol 42:153–184.

Smith FH, Smith MO, Schmitz RW. 2006. Human skeletal remains from the 1997 and 2000 excavations of cave deposits derived from Kleine Feldhofer Grotte in the Neander Valley, Germany. In: Schmitz RW, editor. Neanderthal 1856–2006. Mainz: Zabern. p 187–246.

Terra ER, Guedes FR, Manzi FR, Boscolo FN. 2006. Pneumatization of the sphenoid sinus. Dentomaxillofac Radiol 35:47–49.

Vlcek E. 1967. Die Sinus frontales bei europäischen Neandertalern. Anthropologischer Anzeiger 30:166–189.

Weidenreich F. 1943. The skull of *Sinanthropus pekinensis*: a comparative study of a primitive hominid skull. Palaeontol Sin Ser D 7:1–162.

Weiglein AH. 1999. Development of paranasal sinuses in humans. In: Koppe T, Nagai H, Alt KW, editors. The paranasal sinuses of higher primates. Chicago: Quintessence. p 35–50.

Wind J. 1984. Computerized X-ray tomography of fossil hominid skulls. Am J Phys Anthropol 63:265–282.

Witmer LM. 1999. The phylogenetic history of paranasal air sinuses. In: Koppe T, Nagai H, Alt KW, editors. The paranasal sinuses of higher primates. Chicago: Quintessence. p 21–34.

Zollikofer CPE, Ponce de León MS. 2002. Visualizing patterns of craniofacial shape variation in *Homo sapiens*. Proc Roy Soc B 269:801–807.